Influence of Moisture Diffusion on the Dynamic Compressive Behavior of Glass/Polyester Composite Joints for Marine Engineering Applications

Oumnia Lagdani, Mostapha Tarfaoui, Marwane Rouway, Houda Laaoui, Sara Jamoudi Sbai, Mohamed Dabachi, Abdelwahed Aamir, Mourad Nachtane

Influence of Moisture Diffusion on the Dynamic Compressive Behavior of Glass/Polyester Composite Joints for Marine Engineering Applications

Oumnia Lagdani [1], Mostapha Tarfaoui [1,2], Marwane Rouway [3,4], Houda Laaouidi [1], Sara Jamoudi Sbai [4,5], Mohamed Amine Dabachi [6], Abdelwahed Aamir [7] and Mourad Nachtane [8,*]

1. IRDL Laboratory, ENSTA Bretagne, UMR-CNRS 6027, 29200 Brest, France; oumnialagdani@gmail.com (O.L.); mostapha.tarfaoui@ensta-bretagne.fr (M.T.); laaouidi.h@gmail.com (H.L.)
2. Green Energy Park (IRESEN/UM6P), km 2 R206, Benguerir 43150, Morocco
3. LPMAT Laboratory, FSAC, Hassan II University, Casablanca 20100, Morocco; marwanerouway@gmail.com
4. REMTEX Laboratory, ESITH, Casablanca 20000, Morocco; jamoudi.sa@gmail.com
5. LIMAT Laboratory, FSBM, Hassan II University, Casablanca 20000, Morocco
6. High School of Technology (ESTC), Hassan II University of Casablanca, BP 8012, Casablanca 20000, Morocco; ma.dabachi@ensem.ac.ma
7. MEET Laboratory, FST, Hassan I University, BP 577, Settat 26002, Morocco; profaamir2012@gmail.com
8. Arts et Métiers ParisTech Metz, CNRS, University of Lorraine, LEM3-UMR 7239 CNRS, 57070 Metz, France
* Correspondence: mourad.nachtane@ensta-bretagne.org

Abstract: Thermoset polymers offer great opportunities for mass production of fiber-reinforced composites and are being adopted across a large range of applications within the automotive, aerospace, construction and renewable energy sectors. They are usually chosen for marine engineering applications for their excellent mechanical behavior, including low density and low-cost compared to conventional materials. In the marine environment, these materials are confronted by severe conditions, thus there is the necessity to understand their mechanical behavior under critical loads. The high strain rate performance of bonded joints composite under hygrothermal aging has been studied in this paper. Initially, the bonded composite specimens were hygrothermal aged with the conditions of 50 °C and 80% in temperature and relative humidity, respectively. After that, gravimetric testing is used to describe the moisture diffusion properties for the adhesively bonded composite samples and exhibit lower weight gain for this material. Then, the in-plane dynamic compression experiments were carried out at different impact pressures ranging from 445 to 1240 s^{-1} using the SHPB (Split Hopkinson Pressure Bar) technique. The experimental results demonstrated that the dynamic behavior varies with the variation of strain rate. Buckling and delamination of fiber are the dominant damage criteria observed in the sample during in-plane compression tests.

Keywords: moisture diffusion; compressive behavior; SHPB technique; glass/polyester composite joints

1. Introduction

Glass fiber composites are usually chosen for marine engineering applications due to their excellent mechanical behavior and particularly, their low densities and cost compared to traditional materials [1–5]. However, the most structural requirement of composites is the ability to maintain a high proportion of its load-carrying performance over prolonged time under extreme environmental circumstances, such as temperature changes, humidity, oxidation, microbial attack, etc. [6–8]. Over the past few decades, the strengthening and repair of marine engineering structures using glass fiber reinforced polymer (GFRP) laminates have gained much attention [9,10]. As the science of polymers has advanced, composite bonding has developed into a major joining method for many applications, because it affords a lot of benefits compared to metallic joints, such as high fatigue resistance,

galvanic corrosion elimination and uniform stress distribution across the joint [11–14]. The exploring of the hygrothermal aging effect on the mechanical performance of bonded joints has increasingly become recognized in the last years. The water aging influence on interface debonding has been studied in the literature. Komai et al. [15] demonstrated that water absorption leads to strength loss of the fiber/matrix interfaces of aligned reinforced carbon/epoxy composites. Ashik [16] conducted an experimental study of moisture uptake and mechanical characteristics of hybrid natural and glass fiber reinforced composites. The result shows that the addition of coconut fiber can improve strength and serve as an alternative material to glass fiber. Selzer and Friedrich [17] observed that the bonding of fiber/resin deteriorates with increasing moisture absorption. Due to the individual set of properties that synthetic polymers offer, their applications in the outdoor environment are steadily growing.

Polymers have replaced conventional materials in the marine industry. Many research papers have shown the impact of seawater on polymeric composites which leads to a degradation of performance [18]. Buehler and Seferis [19] noted interface delamination in carbon-glass reinforced epoxy due to water absorption. However, there are limited works on damage mechanisms that can change fatigue resistance, even in the absence of important seawater deterioration. So, it is substantial to better comprehend the extent and mechanisms of seawater deterioration. Schutte [20] demonstrated that hygrothermal decomposition of glass fiber composites is primarily due to the decomposition of the glass fibers, the polymer matrix and the interface. However, Mijović et al. [21] showed that vinylester reinforced composites display excellent durability over epoxy-based composites. Khalilullah [22] characterized the effect of moisture and hygroscopic bulking of silicone/phosphorus composite film, also the moisture uptake with temperature for the film. Therefore, vinylester and epoxy resins are usually chosen due to their low cost, thermal aging resistance and high sustainability [23]. Jiang et al. [24,25] experimentally and numerically investigated the impact of humidity and hygrothermal degradation in GFRP adhesives. The results revealed that samples lost mass under 40 °C conditions. Grace et al. [26] presented a new approach to characterize anisotropic moisture absorption in polymer composites using gravimetric absorption. Benyahia et al. [27] investigated the mechanical behavior of composite pipes at different temperatures between −40 °C and 80 °C where the pipes degrade when temperature increases. Sassi and his colleagues [28–32] investigated the dynamic behavior of bonded composite joints at elevated strain rates using an SHPB machine, the experimental results have shown a strong material sensitivity to strain rates. Moreover, damage investigations have revealed that the failure mainly occurred in the adhesive/adherent interface because of the brittle nature of the polymeric adhesive. Results have shown good agreement with the dependency of the dynamic parameters on strain rates. Despite these efforts, the influence of moisture diffusion on the dynamic compressive behavior of glass/polyester composite joints remains immature. Hence, the importance of understanding the mechanical behavior of these materials that are subjected to critical loads for an extended period. In this context, this paper highlights the impact of hygrothermal aging on the compressive responses of bonded composite joints at an elevated strain rate using the Split Hopkinson Pressure Bar (SHPB) machine.

In summary, the outline of this article is as follows: Section 2 provides the material description and methods, followed by the experimental methodology utilized for the mechanical characterization in Section 3. Finally, Section 4 draws pertinent conclusions as well as some prospects for future developments.

2. Materials and Methods

2.1. Materials

The composite used in this work was made of a 45° biaxial glass fiber mat with 0.29 mm in thickness reinforced polyester polymer. The composite part was joined with an adhesive of polyvinylester with 1 mm in thickness purchased from NORPOL. The mechanical properties of materials are listed in Table 1 [28]. The polyester polymer is

used in the maritime industry as an equivalent to other types of polymers, due to their cost being slightly less than epoxy resin and also it has an excellent performance in corrosive environments and at extreme temperatures; therefore, it is perfectly adapted to naval applications.

**Table 1.** Composite and adhesive mechanical properties.

Properties	Composite	Adhesive
Density (kg/m^3)	1960	1960
Young's modulus (MPa)	E_1 = 48,110, E_2 = E_3 = 11,210	3100
Poisson's ratio	v_{12} = v_{13} = 0.28, v_{23} = 0.34	0.3
Shear modulus (MPa)	G_{12} = G_{13} = 4420, G_{23} = 5000	-

2.2. Methods

2.2.1. Hygrothermal Aging Test

The samples were tested and performed by hygrothermal aging to investigate the moisture absorption properties and to measure the gain in weight of the samples in the function of time. The dimension of samples is 13 mm × 13 mm × 9 mm as shown in Figure 1. To perform the SHPB test, the samples must be prepared where both sides of the specimen are recommended to be planned and oriented with a high level of accuracy. The mass of each sample was calculated every 96 h in a regular period using a Precisa XT220A analytical balance with a tolerance of 0.0001 g. To record the weight variation after a specified interval of time, each specimen is taken out of the conditioned chamber, weighed quickly and returned into the chamber. The moisture uptake M absorbed by each sample is measured as a function of its initial weight w_i and final weight w_f [25,29] as described below:

$$M = \frac{w_f - w_i}{w_i} \times 100 \tag{1}$$
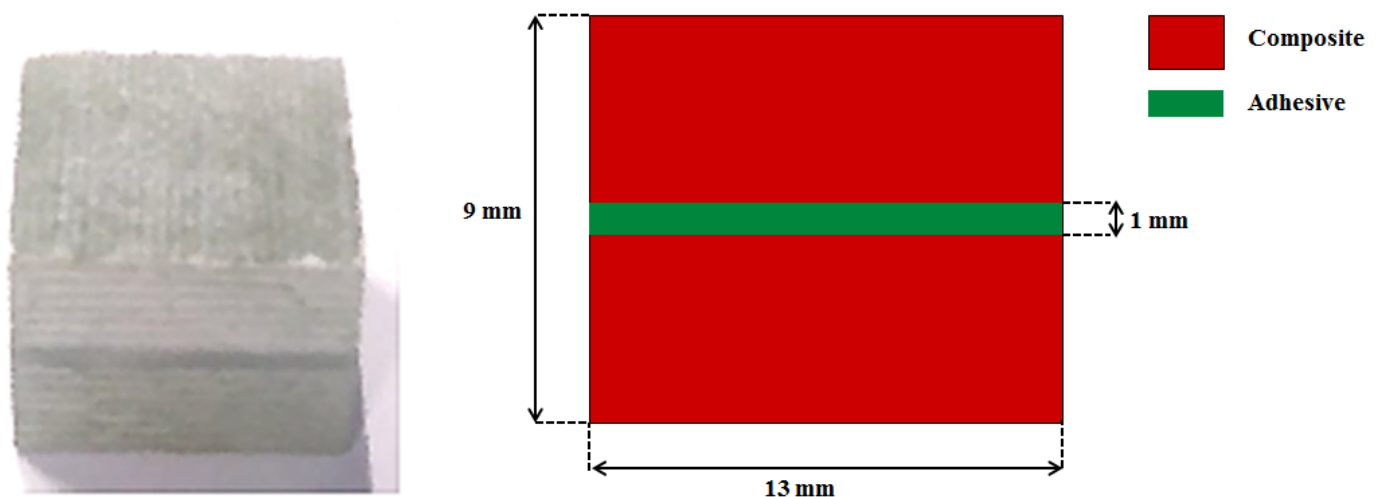
Figure 1. Adhesively bonded composite joints sample.

Before studying the aging of an adhesive, it is necessary to ensure that the polymerization is complete to avoid crosslinking phenomena during aging [2]. The DSC (Differential Scanning Calorimetry) test can determine an adequate curing cycle (polymerization of the glue). Likewise, these tests carried out on polymerized samples make it possible to determine a glass transition temperature T_g. From these data, it is then possible to set aging conditions. In general, it is necessary, for the aging temperature, to be lower than the T_g of an aged material saturated with water to overcome complex aging phenomena in a rubbery state. In addition, it is recommended that the aging temperature be much lower than the post-cure temperature as shown in Figure 2. The bonded composite specimen was

tested under the moisture diffusion effect with 50 °C and 80% of temperature and relative humidity, respectively, for different periods.
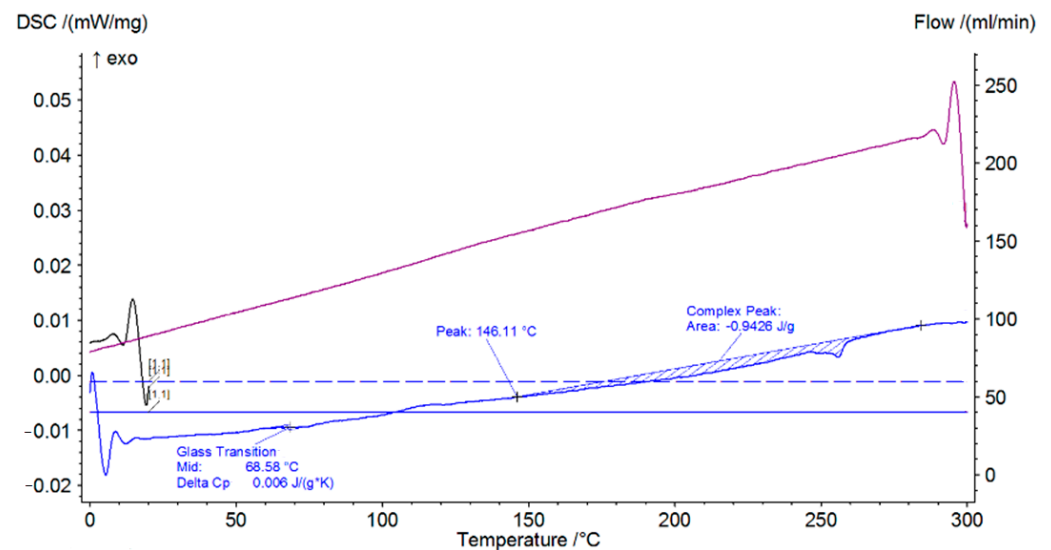

Figure 2. Glass transition temperature of the specimen.

2.2.2. Moisture Absorption

Many researchers investigated the performance degradation of marine water on polymeric composites [30,31]. However, the marine environment could lead to chemical bond hydrolysis and mechanical degradation and also a loss in interfacial stress transmission due to matrix plastification, in addition, the interface changes between the fiber and the matrix [18,32].

Various diffusion models have been developed to comprehend the behavior of homogeneous and heterogeneous materials, the best known and most commonly used of which is the one-dimensional isotropic Fick model [33] as seen in Figure 3, but divergence from this model are frequently remarked. On the other hand, the Langmuir-type model can accurately describe the water absorption of fiber-reinforced epoxy composite [34].

(**a**)   (**b**)
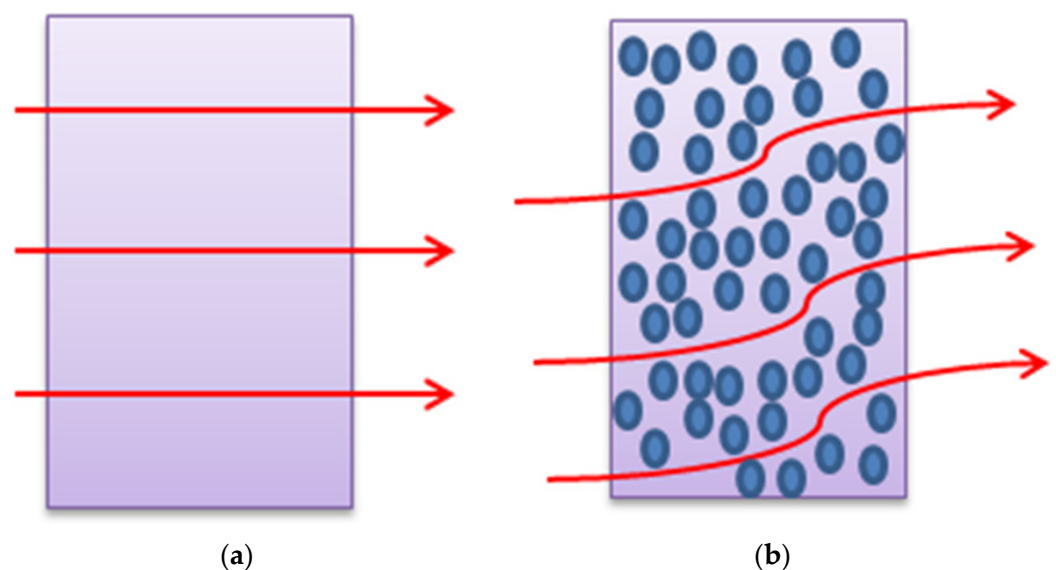
Figure 3. Comparative diagram of diffusion phenomena. (**a**) Homogeneous material, (**b**) Heterogeneous material.

Experimental data were expressed as the moisture uptake $M(t)$. However, the study was conducted using average concentration $C(t)$ as the main parameter. To compare the experimental and numerical results, the $M(t)$ was converted to $C(t)$. The mean concentration was evaluated using Equation (2), where the densities of the material and water at 60 °C are $\rho_{mat} = 1.9$ g/cm^3 and $\rho_{water} = 0.9$ g/cm^3, respectively.

$$C(t) = \frac{\rho_{mat}}{\rho_{eau}} M(t) \qquad (2)$$

The average concentration C_i is computed by using the finite element model at each integration point. So, to compare the results, C_i is evaluated at each increment point for the entire test tube using Equation (3), where C_i and V_i represent the concentration and volume at the integration point, respectively. The equation was executed using a Python script that extracts the appropriate information from the Abaqus results database.

$$C_i(t) = \frac{\sum_{i=1}^{n} C_i V_i}{\sum_{i=1}^{n} V_i} \qquad (3)$$

Figure 4 presents the variation of the moisture uptake curve in the function of the square root of time, which usually concurs with the Fick law. The numerical results remain below the experimental and analytical values which confirm the model correlates satisfactorily with the theoretical and experimental results. The experimental data presented in Figure 4 represents the average of 10 tested samples. The moisture process of bonded joints may be defined into three period phases. In the first phase, the moisture uptake rate grows rapidly with time, achieving to moisture absorption of 0.239 wt% in 49 h. The rate of water absorption in bonded joints was changed linearly with aging time. The moisture uptake in this phase is principal because of composite material defects, such as voids and micro-cracks in the matrix. Into the second phase, the moisture decelerates until the saturation point at 0.2875 wt% in 400 h. The moisture absorption mechanisms include delamination of the fiber/resin interface and hydrolysis of the resin. At the third phase, the moisture diffusion of the composite has achieved equilibrium after approximately 420 h of aging.
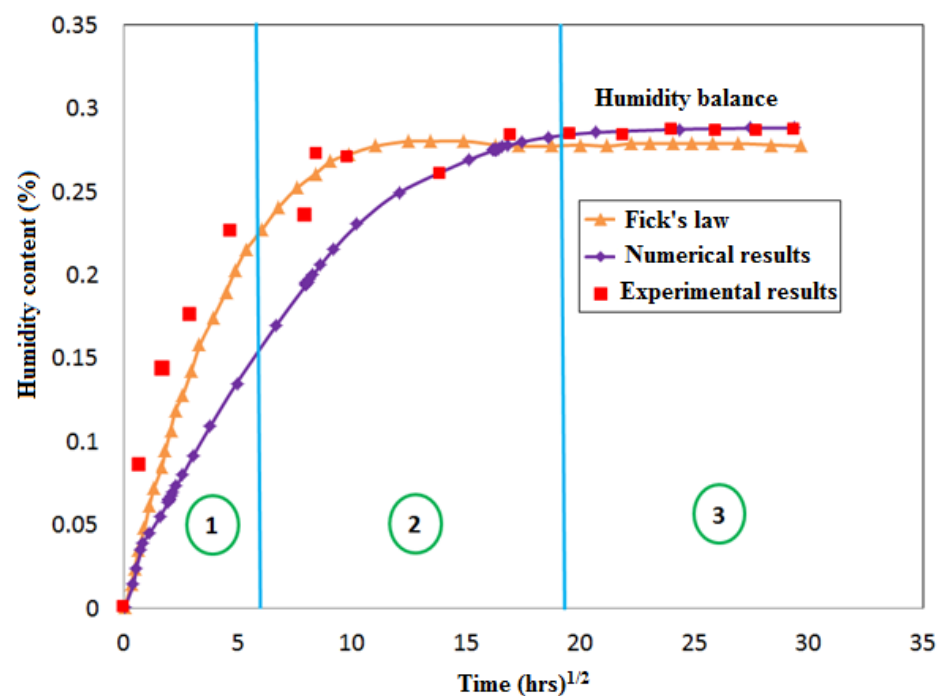
Figure 4. Bonded joint moisture absorption, a comparison of analytical (Fick) and numerical models with experimental data.

Numerous authors have described the volume variation of the specimens under hygrothermal loading. Gazit [35] showed that the increase in sample weight is linearly proportional to the dimensions of all reinforced samples. According to the polarity of water, it can create hydrogen bonds with the hydroxyl groups. Consequently, the hydrogen bonds between chains may be interrupted to raise the length of the hydrogen bond between segments. These mechanisms reduce the glass transition temperature T_g of the wetted specimen and is known as plasticization and swelling of the polymer matrix, which leads to microstructural damage, such as fibers delamination and matrix cracking [36,37]. In contrast, matrix swelling is important in the region with high resin uptake. This induces decoherence of the fiber/resin interface. In another work, Lee [38] demonstrates that the absorption of water produces plasticization and swelling of the resin and a reduction of the glass transition temperature. These generally affect the modulus of the composite material and can be accelerated by increasing the temperature. As observed in Figure 5, the numerical results of moisture diffusion at different aging times (0 h, 216 h, 648 h and 864 h).
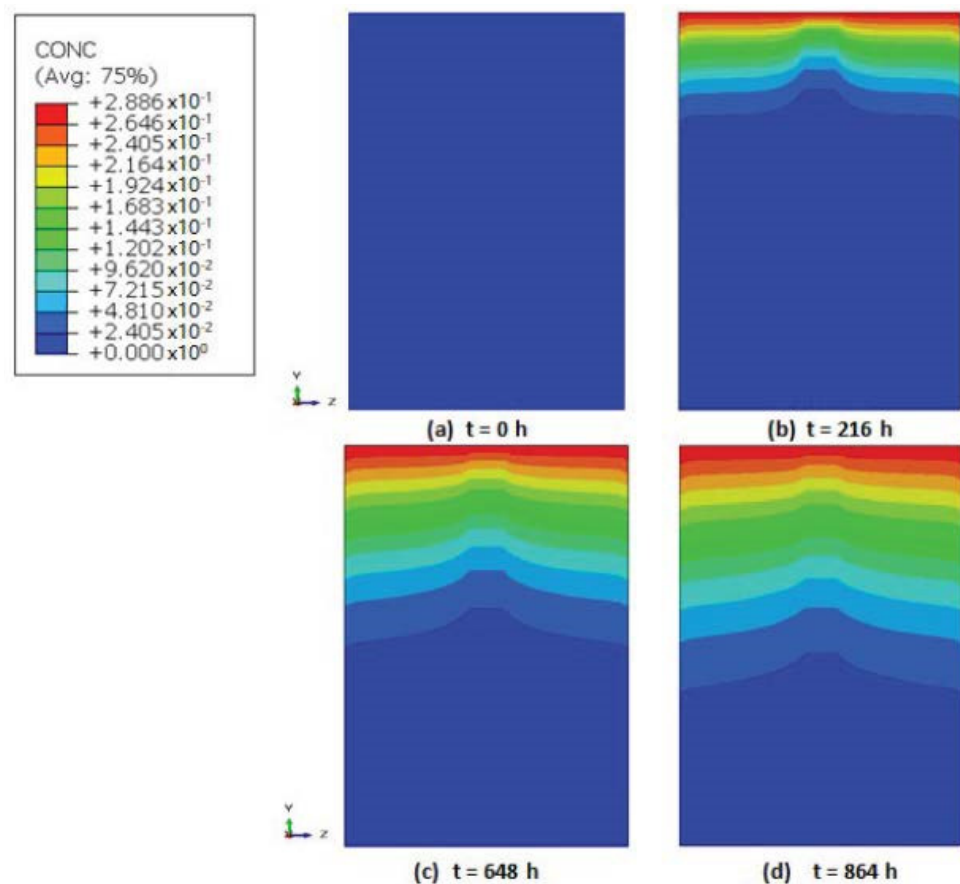

Figure 5. Illustration of numerical results at different aging times.

3. Dynamic Response in Moisture Absorption

3.1. Dynamic Compression Test

Many techniques were employed to evaluate the mechanical characteristics of the composites at high strain rates. The most utilized machines were the Split Hopkinson Pressure Bar (SHPB) for strain rates between 500 and 10^4 s^{-1} [39–41]. Figure 6 illustrates a photograph of the used SHPB machine with different parts of the system including striker bar, input, and output bars. To register the experiment signals, incident and transmitted bars attached with two strain gauges were installed. The samples were embedded between two bars with a diameter of 20 mm in each bar. The striker, input and output bars have a length of 0.8 m, 3 m and 2 m, respectively. The bars are correctly aligned and can move easily on the base. The striker is projected onto the input bar at a specific speed.
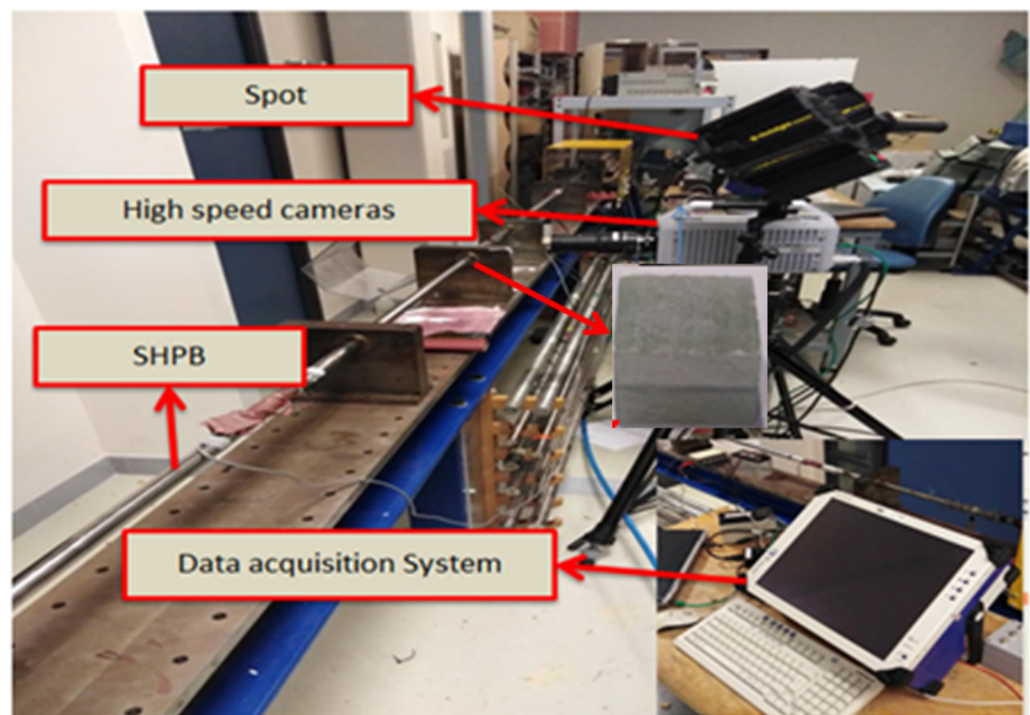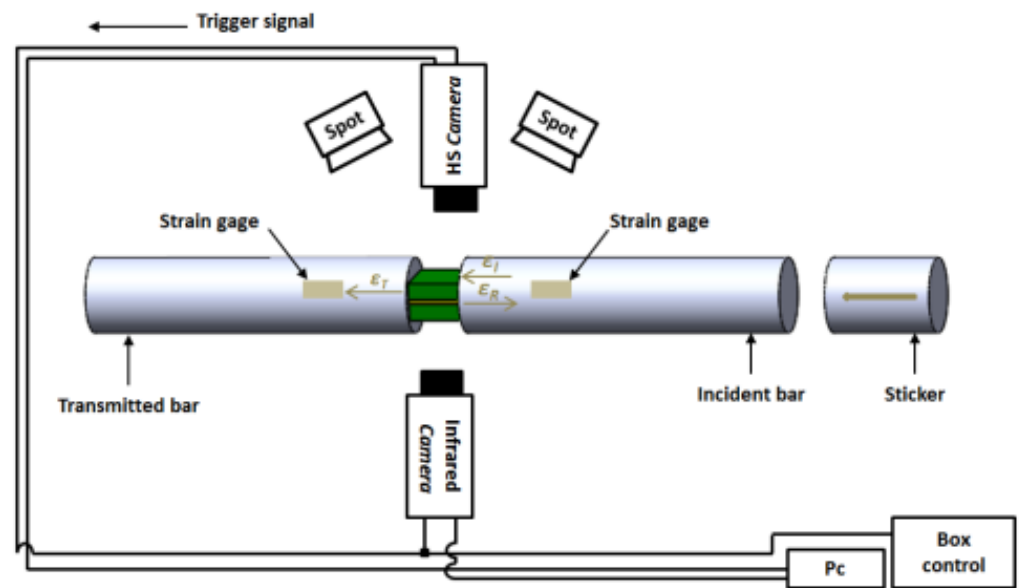
Figure 6. SHPB machine.

3.2. Mechanical Behavior

The thermomechanical properties of a composite are affected by moisture and temperature. However, an increase in moisture and temperature can augment the molecular displacement of the material and can significantly alter the shape and volume of composites. Such deformation is further sophisticated, especially with the dynamic compression of the material. The impact pressure effect on the stress/strain behavior of bonded composite under in-plane dynamic compression is shown in Figure 7.
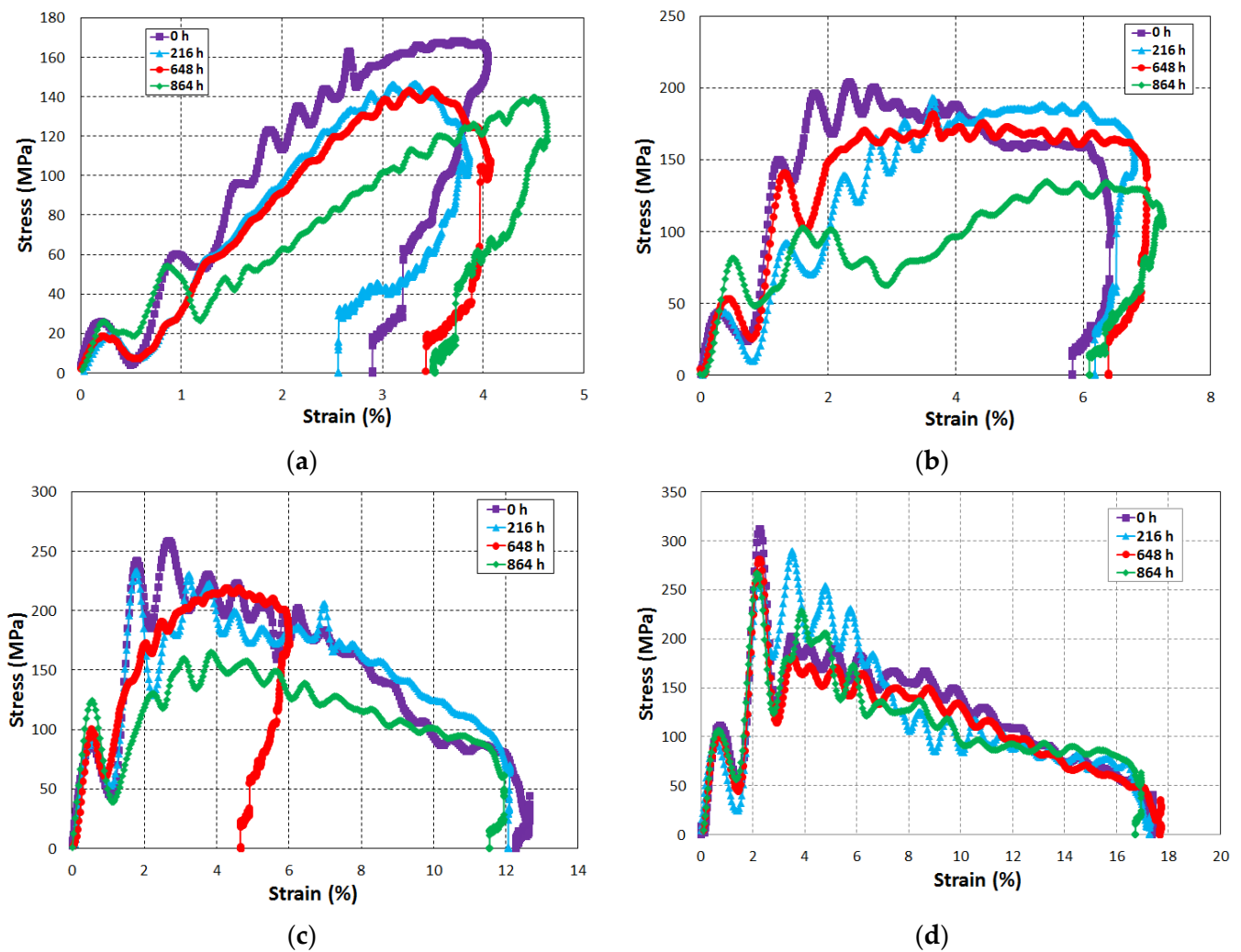
Figure 7. Stress/strain curves of the sample under in-plane loading for different pressure and aging times. (**a**) 1 bar. (**b**) 2 bar. (**c**) 3 bar. (**d**) 4 bar.

Figure 7 presents the stress–strain responses for various impact pressures from 1 bar to 4 bar with various aging times of 0 h, 216 h, 648 h, and 864 h. It can be noted that the dynamic compressive behavior of the composite is strongly affected by strain rate and aging time. Moreover, the effect of moisture on the stress–strain curves is more significant at a low strain rate than at a high strain rate. This clearly shows that the strain rate response is sensitive to the entry pressure P in the chamber of compressed air. At the ultimate stress, the sample damage appears and loses its loadbearing capacity. It is apparent that for all impact tests, the stress–strain tendency was approximately the same during the linear elastic phase, with no damage at small strains. In addition, it can be shown that in the undamaged case, the samples regain their original state with negligible plastic deformation. On the other hand, in the damaged samples, the first peak is observed in the elastic response which shows the beginning of microscopic damage modes, such as matrix cracking. The matrix cracking of samples with in-plan direction encourages micro-buckling and fiber twisting, and leads to debonding, fiber separation, delamination and fiber breaking towards the final failure observed with the appearance of the second peak for the strain rate curves. It can be concluded that the first region of nonlinearity in the stress–strain curves are mainly due to the viscoelastic nature of the polyester polymer, while the nonlinearity noticed before the final failure is caused by the cracking of the matrix, and the elastic modulus reduced with aging time due to the rising of moisture uptake in the composite.

Figure 8 shows the evolution of strain rate as a function of time for different aging times from 0 h to 864 h and with various impact pressures on the bonded joints. It can be observed that the damage becomes significant only for high-pressure impact due to the second peak presented in the signal and it becomes increasingly important as the impact pressure increases, indicating the accumulated failure modes in the material subjected to dynamic loading. In contrast, for low impact pressure, only the residual plastic deformation occurs due to matrix cracks. Thus, the noticeable fact of increasing the strain rate is manifested by changes in the damage modes. The samples tested were damaged by fiber twisting at low strain rates, and by interfacial debonding and delamination at high strain rates.
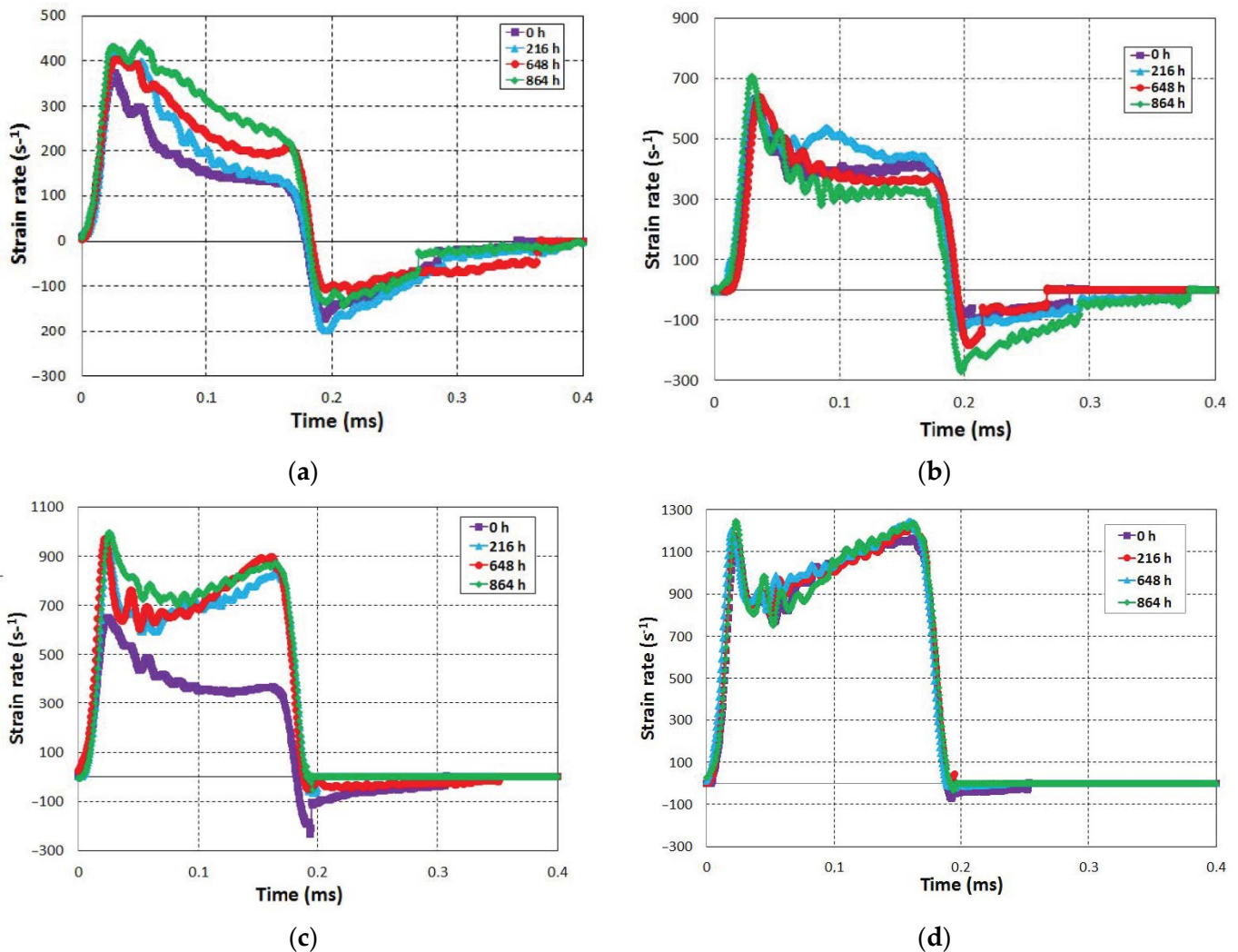
Figure 8. Strain rate versus time curves of the sample at different aging times and pressure under in-plane loading. (**a**) 1 bar. (**b**) 2 bar. (**c**) 3 bar. (**d**) 4 bar.

According to our knowledge, there is no empirical study proposing a constitutive model that reflects the impact of strain rate on bonded joints under dynamic conditions with the effect of aging due to the limited availability of reliable experimental data of dynamic tests. However, the effect of strain rate on the damage of metals and composites has been investigated in many works [42,43]. Many research works have recently been proposed to model the dynamic behavior of the material subjected to impact testing [44,45].

In this paper, empirical laws have been proposed relating to the dependence of the dynamic properties of bonded joints to the impact pressure and strain rate under dynamic in-plane compression loading for different aging times. To optimize the graphical representations, the deformation rate and the maximum stress are given in relation to the

impact pressure. Figure 9 shows the trends obtained from the strain rate dependencies of impact pressure and aging time. The evolution of the strain rate is approximated by a quadratic equation and presents two phases. In the first phase (1 bar $\leq$ P $\leq$ 2 bar) the increase is less pronounced and in the second phase the increase is accelerated. On the other hand, we can see that the stiffness of the material is sensitive to the deformation rate and the aging time. It is to be noticed that these nonlinear equations were derived from empirical plots of the dynamic characterization of specimens for different aging times under dynamic compression. The obtained equations are similar to the quadratic equations of glass/epoxy composite in dynamic compression [42,43]. In addition, Tarfaoui et al. [46] employed the non-linear evaluation of damage versus strain rate for dynamic modeling under pressure impact.
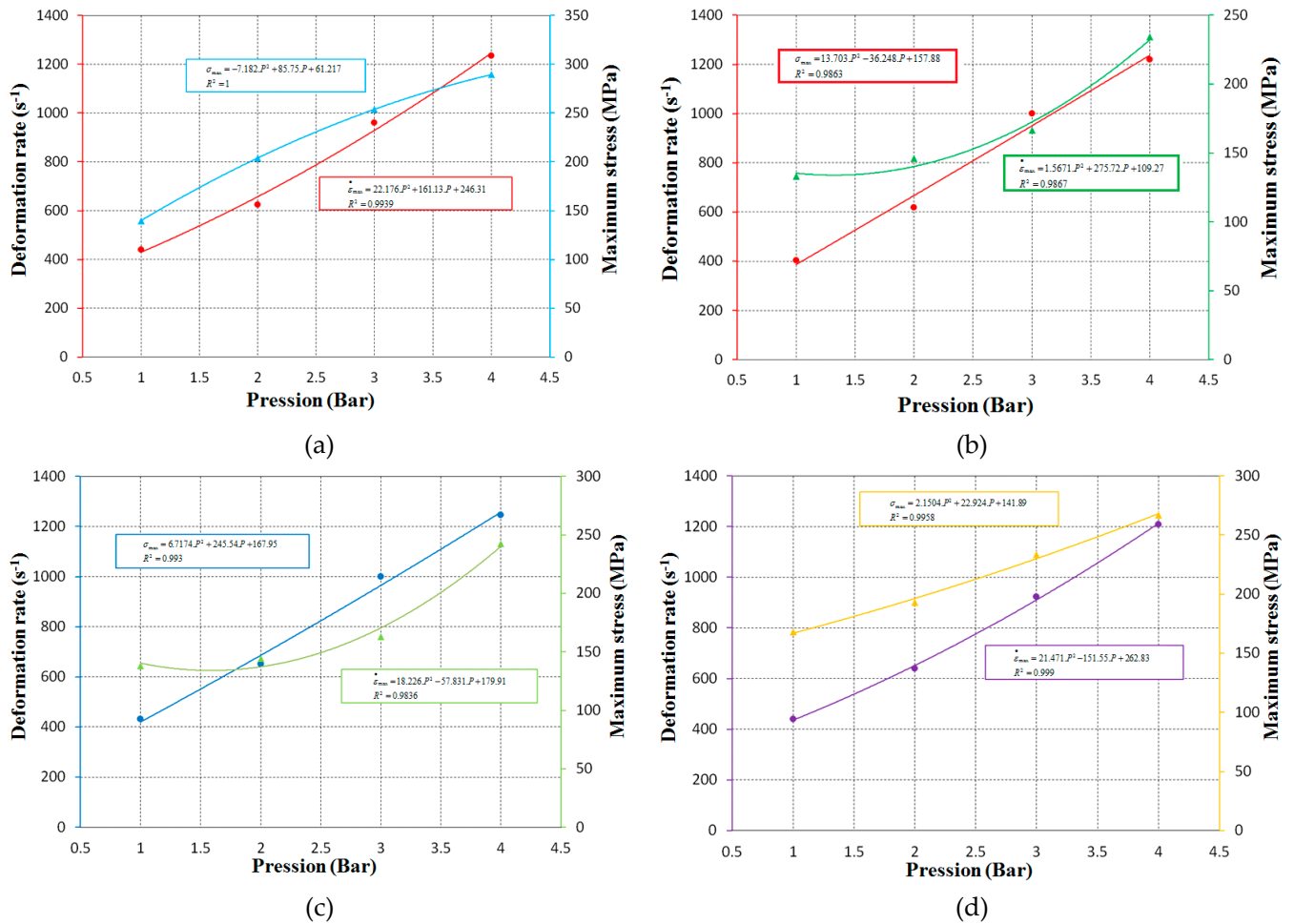
Figure 9. Variation of maximum stress/strain rate in function of aging time. (**a**) $t = 0$ h. (**b**) $t = 216$ h. (**c**) $t = 648$ h. (**d**) $t = 864$ h.

3.3. Theoretical Characterization of Absorbed Energy

The incident impact energy is the complete energy available at the start and represents the kinetic energy contributed by the impactor. At the interface between the bar and sample, a portion of this energy is absorbed by the specimen and can produce damage or plastic deformation in various forms and also can generate heat, which is associated with the occurrence of microscopic/macroscopic damage. The rest of the energy consists of reflected and transmitted energy and can be measured from the deformation profile. The absorbed energy W_{abs} is expressed as follows:

$$W_{abs} = W_{inc} - (W_{trans} - W_{ref}) \tag{4}$$

With W_{inc}, W_{ref} and W_{trans} representing the incident, reflected and transmitted energy, respectively, and their expressions are given by:

$$W_{inc} = \frac{A}{\rho c} \int_0^t \sigma_i^2(t)dt \tag{5}$$

$$W_{ref} = \frac{A}{\rho c} \int_0^t \sigma_r^2(t)dt \tag{6}$$

$$W_{trans} = \frac{A}{\rho c} \int_0^t \sigma_t^2(t)dt \tag{7}$$

Figure 10 presents typical absorbed energy by the sample at an impact pressure of 4 bar for an aging time of t = 648 h. The energy versus time curves representative of the aged bonded joint sample indicates that the incident and reflected energy increases quickly compared to the transmitted and absorbed energy during the propagation of the deformation wave and their values are maintained stable after achieving a required value, and the apparition of the maximum absorption energy indicating the presence of damage to the joint. Much research indicates that there is a relationship between damage modes and the characteristics of the absorbed energy [47]. The results demonstrated that the impact energy can influence the absorbed energy and can be described as follows:

- As the impact energy increases, the number of damage cracks is large and its distribution becomes more uniform, while the energy absorbed also increases as shown in Figure 10.
- Most of the incident energy is absorbed due to the effect of aging and the low impedance of composites.
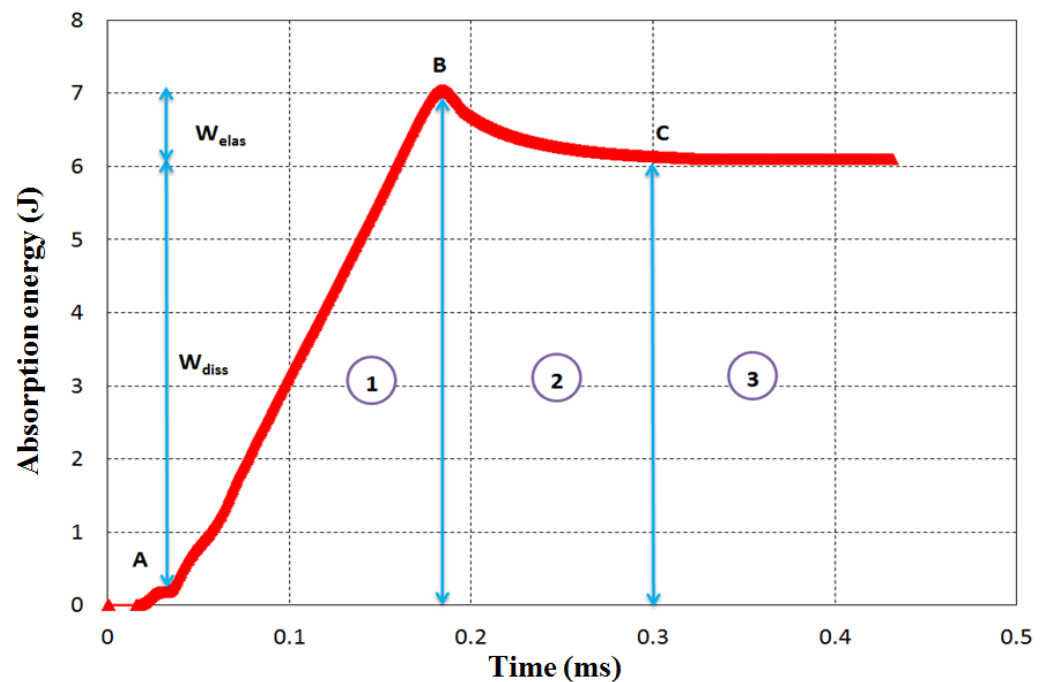
Figure 10. Typical profile of absorbed energy W_{abs}.

Moreover, the incident energy in the initial part increases quickly with the stress wave propagation, whereas the absorbed energy of the bonded joint has a small increase with the propagation of the stress wave. This is because the majority of the incident energy is absorbed by the specimens and just a minor fraction of the incident energy is transferred into the transmitted bar. In Figure 10, the presence of different zones can be identified:

- Zone 1 represents the loading phase (AB): The sample is absorbing energy at point B ($W_{abs} = y_B - y_A$), and this energy is composed of an elastic component and an unrecovered dissipative component.
- Zone 2 represents the progressive discharge part: The elastic energy is realized up to point C ($W_{elas} = y_B - y_C$).
- Zone 3 represents the final stage of the charge/discharge cycle: W_{abs} corresponds to the energy permanently dissipated in the material.

In this way, the absorbed energy is decomposed into an unrecovered elastic part and an inelastic part, and can be expressed by the equation below:

$$W_{abs} = W_{elas} + W_{diss} \tag{8}$$

W_{abs} is the energy absorbed by the sample other than the stored deformation energy that is exhausted to create damage. The inelastic part is related to the damage generation in different forms, such as matrix fracture, fiber rupture, and delamination or decohesion between the fiber and matrix. The curve of the absorbed energy tends towards a fixed value at the end of the first cycle where the transmitted signal is reflected by the incident, and permanently corresponds to the energy dissipated by the damage in the sample. Figure 11 shows the absorption energy for a compression test for an aging time of 216 h at different impact pressures. The fluctuating profiles represent the release and storage of deformation energy throughout the experimental process. It can be easily observed that at low impact energy, a considerable amount of the input energy of W_{elas} is stored in the loading phase and released in the discharge phase. On the other hand, W_{abs} has an increase as the impact pressure is raised, which in turn influences the release of W_{elas} through the discharge phase. The last one (W_{elas}) is the largest fraction of W_{abs} at low impact energy, while W_{diss} takes a larger fraction of W_{abs} as the impact energy increases. It should be noted that W_{elas} is zero when the sample has macroscopic damage. One can also note that the loading portions of the curves for the several impact pressures are coherent and overlapped. Additionally, an increase is observed in slope with the increase of impact pressure, with the suggestion that the reaction is conditioned by the deformation rate.
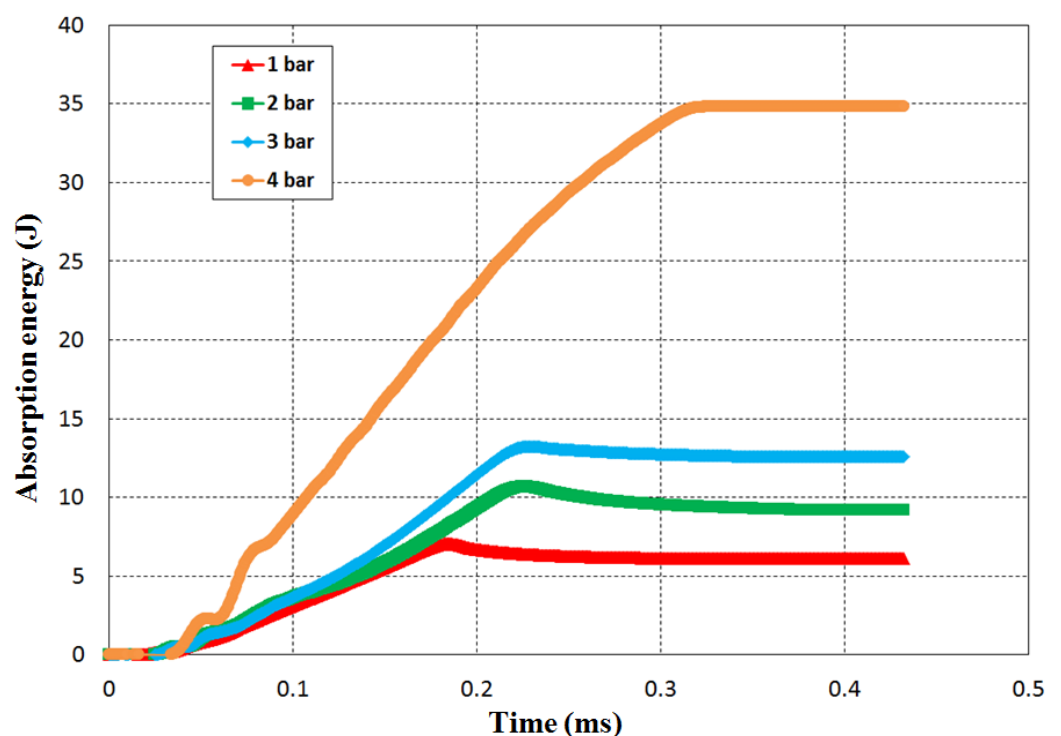

**Figure 11.** Absorbed energy for an aging time *t* = 216 h.

3.4. Damage Mechanisms and Failure Modes

A camera with a high-speed system is employed to visualize the damage mode of the samples. Figure 12 shows the damage pattern of the bonded composite loaded in an in-plane direction. It can be noted that the damage is observed as cracks across the diagonal of the cube. In addition, matrix fractures and intense delamination are produced in the preferred inter-laminar planes. To understand the damage behavior of the bonded joined under dynamic loading, a camera of high-speed is used to capture the loading of the sample at different impact pressures. The damage is observed only at high impact pressures. For low impact pressure, only residual plastic deformations due to matrix fractures were present. So as the damage mechanism is developed, it is expressed in the form of matrix/fiber failure, fiber pullout, and delamination of the ply pack.

| 1 bar | 2 bar | 3 bar | 4 bar |

Elevated Pressure
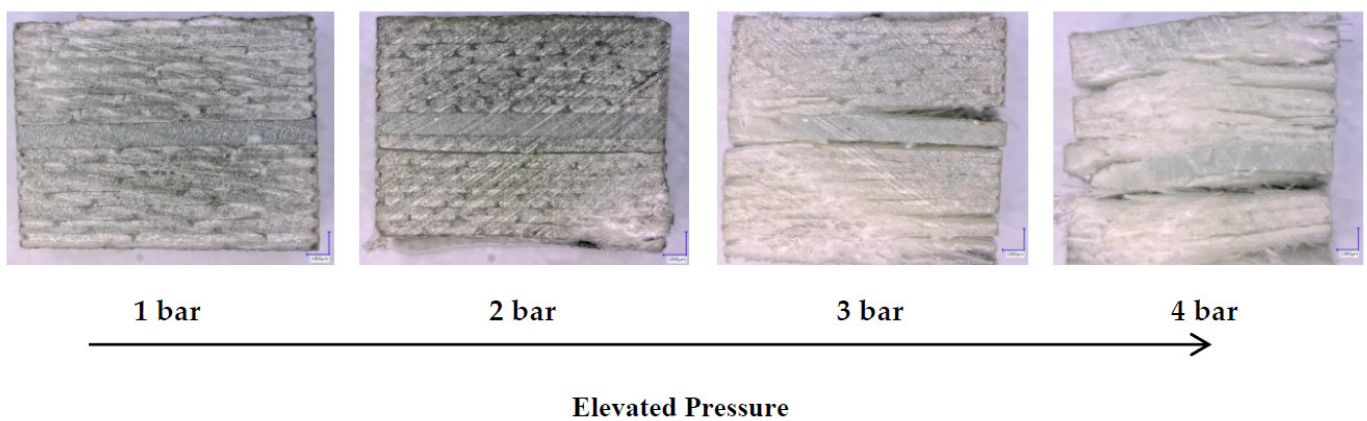
Figure 12. Optical micrographs of bonded composite under dynamic compression for *t* = 216 h.
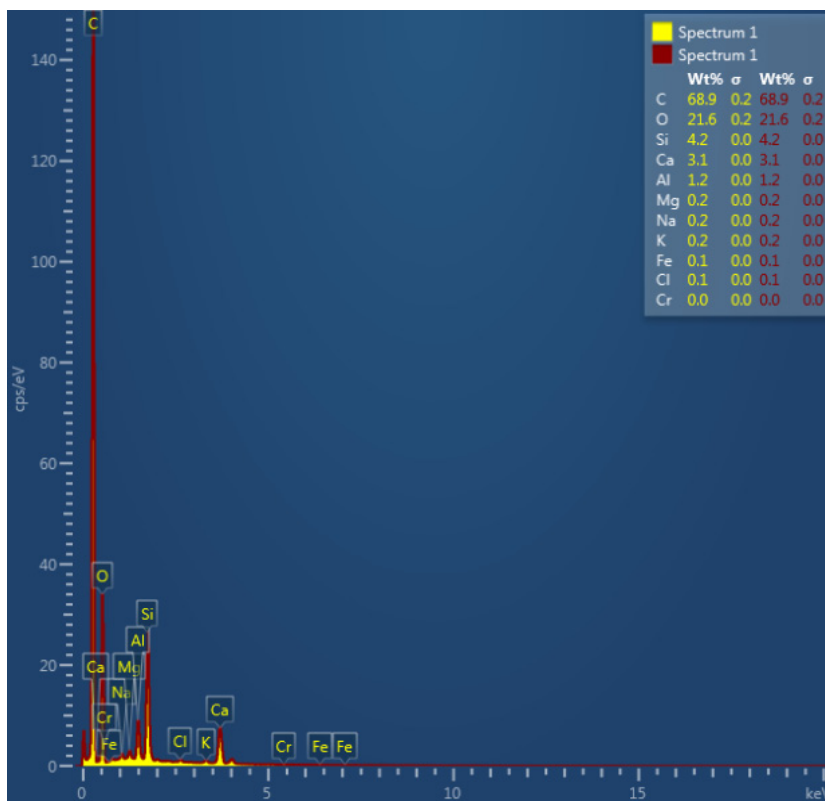
The fiber and matrix can be observed to be highly bonded before hygrothermal aging. The beginning of the damage includes a "V" shaped shear band and the development of delamination at its tip. Microcracks were observed at the interface of matrix/fiber after 216 h, as shown in Figure 13. By increasing the hygrothermal aging time, the interface disbonding grows and propagates as long cracks at the 864 h aging time. The obvious interfacial degradation effects of moisture absorbed in the bonded composites on the interfacial area between the adhesive and the composite are detected. In these results, the hygrothermal influence causes chemical changes in the resin matrix, plasticization and dimensional changes, such as swelling, and deterioration of the strength of the adhesive/composite interface. The bond between the fiber and matrix weakens and the interface weakens as the moisture absorption increases. All these factors reduce the impact resistance of the composite.
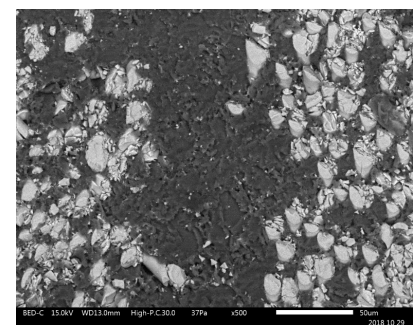

| 0 h | 216 h | 648 h | 864 h |

Increasing Soaking Period
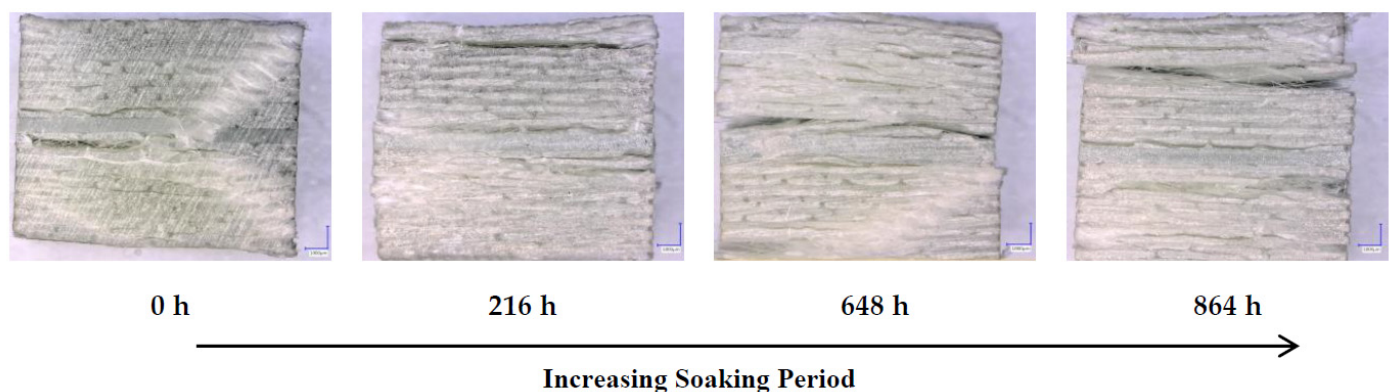
Figure 13. Optical micrographs of adhesively bonded composite loaded through at pressure of 3 bar.

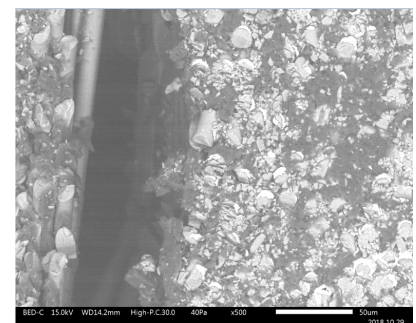*3.5. Microstructural Analysis of Adhesively Bonded Composite*

Figure 14 illustrates the microstructure of adhesive bonded composite as remarked using SEM. There were no significant morphological differences. The materials contain the elements of C, O, Mg, Al, Si, K and Ca. It is observed that the crack propagation rate of bonded composite joints becomes more prominent with the increase in strain rate. The results of reaching such raised strength and initial modulus can be justified by the fact that the composite materials become comparatively brittle and harder, which leads to high strength and modulus [36]. The results show also that the failure stresses degrade for various aging times for the samples subjected to in-plane compression because temperature and humidity considerably modify and weaken the composite. The strain rate is seen to be increased for various aging times. These results can be explained by the plasticization of the matrix being the principal factor in high strain rate properties when materials are not totally immersed in corrosion enclosure. Therefore, the matrix is more responsive to the strain rate and thus, plays a more important role than the fiber in identifying the material performance response to the high strain rate of polymer matrix composites. From the above discussion, it is further revealed that the crack propagation model changes as the deformation rate increases, and the higher the deformation rate, the more complex the crack propagation model appears.

Virgin sample

Damaged sample at 3 bar

Damaged sample at 4 bar

EDS spectra of damage (spectrum 1) and undamaged (spectrum 2) adhesive bonded composite

Figure 14. SEM micrographs of the composite of bonded adhesive at 864 h.

4. Conclusions

In the present paper, the influence of moisture diffusion on the dynamic compressive behavior of glass/polyester composite was investigated. The failure modes were viewed by SEM and scanning electron microscopy for different aged specimens. The results obtained show that the hygrothermal influence induces chemical changes in the resin matrix, plasticization and dimensional changes, such as swelling, and also the weakened adhesive/composite interfaces. In addition, the bond between the fiber and the matrix is weakened as the humidity uptake increases. All of these elements would affect the dynamic behavior and the impact strength of an assembly of composite materials. The conclusions from this investigation can be summarized as follows:

1. Matrix plasticization is the major factor in the high strain rate properties when materials are partially or fully wet-immersed in a room temperature bath.
2. The matrix is more sensitive to deformation rate, and therefore, plays a more important role than the fiber in identifying the high deformation rate material behavior of polymer matrix composites.
3. The deterioration of the interface fiber/matrix leads to a decrease in the favorable impact of the plasticization of the matrix.
4. An overall increase in material properties occurs due to absorption of moisture, except in high-temperature baths, due to the extreme degradation of the interface.
5. There is an amount of absorbed moisture that gives optimum material properties that correspond to the highest matrix plasticization with minimal degradation of the interface between fiber and matrix.

Author Contributions: O.L.: Investigation, Methodology, Writing—original draft; M.T.: Methodology, Investigation, Project administration, Conceptualization, Writing—original draft, Writing—review & editing, Funding acquisition; M.R. Methodology, Investigation, Writing—original draft, Writing—review & editing; H.L., S.J.S., M.A.D., A.A.: Validation, Visualization; M.N.: Methodology, Investigation, Writing—original draft, Writing—review & editing, Conceptualization, Data curation, Supervision, Validation, Visualization. All authors have read and agreed to the published version of the manuscript.

Institutional Review Board Statement: Not applicable.

Informed Consent Statement: Not applicable.

Conflicts of Interest: The authors declare no conflict of interest.

References

1. Nachtane, M.; Tarfaoui, M.; Saifaoui, D.; El Moumen, A.; Hassoon, O.H.; Benyahia, H. Evaluation of Durability of Composite Materials Applied to Renewable Marine Energy: Case of Ducted Tidal Turbine. *Energy Rep.* **2018**, *4*, 31–40. [CrossRef]
2. Mangalgiri, P.D. Composite Materials for Aerospace Applications. *Bull. Mater. Sci.* **1999**, *22*, 657–664. [CrossRef]
3. Nachtane, M.; Tarfaoui, M.; Saifaoui, D.; El Moumen, A.; Boudounit, H. Caractérisation Mécanique d'une Hydrolienne En Matériau Composite Dans Un Environnement Marin. In Proceedings of the 2017 23e Congrès français de Mécanique-CFM, Lille, France, 28 August–1 September 2017; Association Française de Mécanique (AFM): Courbevoie, France, 2017.
4. Nachtane, M.; Tarfaoui, M.; El Moumen, A.; Saifaoui, D. Numerical Investigation of Damage Progressive in Composite Tidal Turbine for Renewable Marine Energy. In Proceedings of the 2016 International Renewable and Sustainable Energy Conference (IRSEC), Marrakech, Morocco, 14–17 November 2016; pp. 559–563.
5. Nachtane, M.; Tarfaoui, M.; Goda, I.; Rouway, M. A Review on the Technologies, Design Considerations and Numerical Models of Tidal Current Turbines. *Renew. Energy* **2020**, *157*, 1274–1288. [CrossRef]
6. Maziz, A.; Tarfaoui, M.; Gemi, L.; Rechak, S.; Nachtane, M. A Progressive Damage Model for Pressurized Filament-Wound Hybrid Composite Pipe under Low-Velocity Impact. *Compos. Struct.* **2021**, *276*, 114520. [CrossRef]
7. Maziz, A.; Tarfaoui, M.; Rechak, S.; Nachtane, M.; Gemi, L. Finite Element Analysis of Impact-Induced Damage in Pressurized Hybrid Composites Pipes. *Int. J. Appl. Mech.* **2021**, *13*, 2150074. [CrossRef]
8. Nachtane, M.; Tarfaoui, M.; Ledoux, Y.; Khammassi, S.; Leneveu, E.; Pelleter, J. Experimental Investigation on the Dynamic Behavior of 3D Printed CF-PEKK Composite under Cyclic Uniaxial Compression. *Compos. Struct.* **2020**, *247*, 112474. [CrossRef]

9. Shahawy, M.A.; Beitelman, T.; Arockiasamy, M.; Sowrirajan, R. Experimental Investigation on Structural Repair and Strengthening of Damaged Prestressed Concrete Slabs Utilizing Externally Bonded Carbon Laminates. *Compos. Part B Eng.* **1996**, *27*, 217–224. [CrossRef]

10. Nachtane, M.; Tarfaoui, M.; El Moumen, A.; Saifaoui, D. Damage Prediction of Horizontal Axis Marine Current Turbines under Hydrodynamic, Hydrostatic and Impacts Loads. *Compos. Struct.* **2017**, *170*, 146–157. [CrossRef]

11. Sassi, S.; Tarfaoui, M.; Yahia, H.B. In-Situ Heat Dissipation Monitoring in Adhesively Bonded Composite Joints under Dynamic Compression Loading Using SHPB. *Compos. Part B Eng.* **2018**, *154*, 64–76. [CrossRef]

12. Sassi, S.; Tarfaoui, M.; Yahia, H.B. Thermomechanical Behavior of Adhesively Bonded Joints under Out-of-Plane Dynamic Compression Loading at High Strain Rate. *J. Compos. Mater.* **2018**, *52*, 4171–4184. [CrossRef]

13. Laaouidi, H.; Tarfaoui, M.; Nachtane, M.; Lagdani, O. Modal Analysis of Composite Nozzle for an Optimal Design of a Tidal Current Turbine. *J. Nav. Archit. Mar. Eng.* **2021**, *18*, 39–54.

14. Lagdani, O.; Tarfaoui, M.; Nachtane, M.; Trihi, M.; Laaouidi, H. Modal Analysis of an Iced Offshore Composite Wind Turbine Blade. *Wind Eng.* **2021**, *46*, 134–149. [CrossRef]

15. Komai, K.; Minoshima, K.; Shibutani, T.; Nomura, T. The Influence of Water on the Mechanical Properties and Fatigue Strength of Angle-Ply Carbon/Epoxy Composites. *JSME Int. J. Ser. 1 Solid Mech. Strength Mater.* **1989**, *32*, 588–595. [CrossRef]

16. Ashik, K.P.; Sharma, R.S.; Guptha, V.J. Investigation of Moisture Absorption and Mechanical Properties of Natural/Glass Fiber Reinforced Polymer Hybrid Composites. *Mater. Today Proc.* **2018**, *5*, 3000–3007. [CrossRef]

17. Selzer, R.; Friedrich, K. Inluence of Water Up-Take on Interlaminar Fracture Properties of Carbon Fibre-Reinforced Polymer Composites. *J. Mater. Sci.* **1995**, *30*, 334–338. [CrossRef]

18. Wu, L.; Hoa, S.V.; Ton-That, M.-T. Effects of Water on the Curing and Properties of Epoxy Adhesive Used for Bonding FRP Composite Sheet to Concrete. *J. Appl. Polym. Sci.* **2004**, *92*, 2261–2268. [CrossRef]

19. Buehler, F.U.; Seferis, J.C. Effect of Reinforcement and Solvent Content on Moisture Absorption in Epoxy Composite Materials. *Compos. Part A Appl. Sci. Manuf.* **2000**, *31*, 741–748. [CrossRef]

20. Schutte, C.L. Environmental Durability of Glass-Fiber Composites. *Mater. Sci. Eng. R Rep.* **1994**, *13*, 265–323. [CrossRef]

21. Mijović, J.; Zhang, H. Molecular Dynamics Simulation Study of Motions and Interactions of Water in a Polymer Network. *J. Phys. Chem. B* **2004**, *108*, 2557–2563. [CrossRef]

22. Khalilullah, I.; Reza, T.; Chen, L.; Mazumder, A.M.H.; Fan, J.; Qian, C.; Zhang, G.; Fan, X. In-Situ Characterization of Moisture Absorption and Hygroscopic Swelling of Silicone/Phosphor Composite Film and Epoxy Mold Compound in LED Packaging. In Proceedings of the 2017 18th International Conference on Thermal, Mechanical and Multi-Physics Simulation and Experiments in Microelectronics and Microsystems (EuroSimE), Dresden, Germany, 3–5 April 2017; Institute of Electrical and Electronics Engineers IEEE: Piscataway Township, NJ, USA, 2017; pp. 1–9.

23. Megel, M.; Kumosa, L.; Ely, T.; Armentrout, D.; Kumosa, M. Initiation of Stress-Corrosion Cracking in Unidirectional Glass/Polymer Composite Materials. *Compos. Sci. Technol.* **2001**, *61*, 231–246. [CrossRef]

24. Jiang, X.; Kolstein, H.; Bijlaard, F.; Qiang, X. Effects of Hygrothermal Aging on Glass-Fibre Reinforced Polymer Laminates and Adhesive of FRP Composite Bridge: Moisture Diffusion Characteristics. *Compos. Part A Appl. Sci. Manuf.* **2014**, *57*, 49–58. [CrossRef]

25. Nachtane, M.; Tarfaoui, M.; Saifaoui, D.; Hilmi, K. Hygrothermal and Mechanical Performance Evaluation of Glass-Polyester Composite for Renewable Marine Energies. In Proceedings of the 13ème Congrès de Mécanique (cmm2017), Meknès, Morocco, 4–11 April 2017.

26. Grace, L.R.; Altan, M.C. Characterization of Anisotropic Moisture Absorption in Polymeric Composites Using Hindered Diffusion Model. *Compos. Part A Appl. Sci. Manuf.* **2012**, *43*, 1187–1196. [CrossRef]

27. Benyahia, H.; Tarfaoui, M.; El Moumen, A.; Ouinas, D.; Hassoon, O.H. Mechanical Properties of Offshoring Polymer Composite Pipes at Various Temperatures. *Compos. Part B Eng.* **2018**, *152*, 231–240. [CrossRef]

28. Sassi, S.; Tarfaoui, M.; Yahia, H.B. An Investigation of In-Plane Dynamic Behavior of Adhesively-Bonded Composite Joints under Dynamic Compression at High Strain Rate. *Compos. Struct.* **2018**, *191*, 168–179. [CrossRef]

29. Firdosh, S.; Murthy, H.N.; Angadi, G.; Raghavendra, N. Investigation of Water Absorption Characteristics of Nano-Gelcoat for Marine Application. *Prog. Org. Coat.* **2018**, *114*, 173–187. [CrossRef]

30. Shah, O.R.; Tarfaoui, M. Effect of Damage Progression on the Heat Generation and Final Failure of a Polyester–Glass Fiber Composite under Tension–Tension Cyclic Loading. *Compos. Part B Eng.* **2014**, *62*, 121–125. [CrossRef]

31. Hassoon, O.H.; Tarfaoui, M.; Alaoui, A.E.M.; El Moumen, A. Experimental and Numerical Investigation on the Dynamic Response of Sandwich Composite Panels under Hydrodynamic Slamming Loads. *Compos. Struct.* **2017**, *178*, 297–307. [CrossRef]

32. Gargano, A.; Pingkarawat, K.; Pickerd, V.; Delaney, T.; Das, R.; Mouritz, A.P. Effect of Seawater Immersion on the Explosive Blast Response of a Carbon Fibre-Polymer Laminate. *Compos. Part A Appl. Sci. Manuf.* **2018**, *109*, 382–391. [CrossRef]

33. Pang, S.; Tao, W.; Liang, Y.; Liu, Y.; Huan, S. A Modified Method of Pulse-Shaper Technique Applied in SHPB. *Compos. Part B Eng.* **2019**, *165*, 215–221. [CrossRef]

34. Zhao, H.; Gary, G. On the Use of SHPB Techniques to Determine the Dynamic Behavior of Materials in the Range of Small Strains. *Int. J. Solids Struct.* **1996**, *33*, 3363–3375. [CrossRef]

35. Gazit, S. Dimensional Changes in Glass-Filled Epoxy Resin as a Result of Absorption of Atmospheric Moisture. *J. Appl. Polym. Sci.* **1978**, *22*, 3547–3558. [CrossRef]

36. Haque, A.; Hossain, M.K. Effects of Moisture and Temperature on High Strain Rate Behavior of S2-Glass–Vinyl Ester Woven Composites. *J. Compos. Mater.* **2003**, *37*, 627–647. [CrossRef]
37. Sassi, S.; Tarfaoui, M.; Nachtane, M.; Ben Yahia, H. Strain Rate Effects on the Dynamic Compressive Response and the Failure Behavior of Polyester Matrix. *Compos. Part B Eng.* **2019**, *174*, 107040. [CrossRef]
38. Lee, M.C.; Peppas, N.A. Water Transport in Graphite/Epoxy Composites. *J. Appl. Polym. Sci.* **1993**, *47*, 1349–1359. [CrossRef]
39. Khosravani, M.R.; Weinberg, K. A Review on Split Hopkinson Bar Experiments on the Dynamic Characterisation of Concrete. *Constr. Build. Mater.* **2018**, *190*, 1264–1283. [CrossRef]
40. Tarfaoui, M.; Nachtane, M. Can a Three-Dimensional Composite Really Provide Better Mechanical Performance Compared to Two-Dimensional Composite under Compressive Loading? *J. Reinf. Plast. Compos.* **2019**, *38*, 49–61. [CrossRef]
41. Nachtane, M. Staking Lay-up Effect on Dynamic Compression Behaviour of e-Glass/Epoxy Composite Materials: Experimental and Numerical Investigation. *Adv. Mater. Lett.* **2018**, *9*, 816–822.
42. Randles, P.W.; Nemes, J.A. A Continuum Damage Model for Thick Composite Materials Subjected to High-Rate Dynamic Loading. *Mech. Mater.* **1992**, *13*, 1–13. [CrossRef]
43. Park, S.W.; Schapery, R.A. A Viscoelastic Constitutive Model for Particulate Composites with Growing Damage. *Int. J. Solids Struct.* **1997**, *34*, 931–947. [CrossRef]
44. Li, Y.; Ramesh, K.T.; Chin, E.S.C. Viscoplastic Deformations and Compressive Damage in an A359/SiCp Metal–Matrix Composite. *Acta Mater.* **2000**, *48*, 1563–1573. [CrossRef]
45. Yang, L.M.; Shim, V.P.W.; Lim, C.T. A Visco-Hyperelastic Approach to Modelling the Constitutive Behaviour of Rubber. *Int. J. Impact Eng.* **2000**, *24*, 545–560. [CrossRef]
46. Tarfaoui, M.; Choukri, S.; Neme, A. Effect of Fibre Orientation on Mechanical Properties of the Laminated Polymer Composites Subjected to Out-of-Plane High Strain Rate Compressive Loadings. *Compos. Sci. Technol.* **2008**, *68*, 477–485. [CrossRef]
47. Liu, D.; Schulz, P.; Templeton, D.; Raju, B. Dynamic Failure and Energy Absorption of Composite Materials with Geometrical Control. In Proceedings of the 16th International Conference on Composite Materials, Kyoto, Japan, 8–13 July 2007.